

Explore the Application of Waste Gypsum in Intelligent Construction

Yang Wen¹, Zixin Ai^{2,*} and Yaoyu Wang¹

¹Key Laboratory for Prediction & Control on Complicated Structure System of the Education Department of Liaoning Province, Dalian University, Dalian 116622, China

²School of Transportation Engineering, Dalian Jiaotong University, Dalian 116622, China


Keywords: Phosphogypsum, 3D Printing, Mechanical Properties, Resource Utilization.


Abstract: This study explores the potential application of waste gypsum, particularly phosphogypsum (PG) in the field of intelligent construction. Through calcination pretreatment and 3D printing technology, the physical and chemical properties of phosphogypsum and their impact on 3D printing performance were investigated. Initially, the chemical composition and microstructure of the raw phosphogypsum were analyzed using X-ray fluorescence spectrometer (XRF), X-ray diffractometer (XRD), and scanning electron microscope (SEM). Subsequently, the effect of different calcination temperatures on the dehydration reaction and phase composition of phosphogypsum was studied through calcination treatment. Then, using 3D printing technology, the influence of different water-to-cement ratios (w/c) on the printability and mechanical properties of phosphogypsum paste was explored. The results indicated that the dehydration reaction of phosphogypsum was most significant at a calcination temperature of 175°C, and the 3D printing effect of phosphogypsum paste was optimal at w/c = 0.67, with the printed components being continuous, uniform, and smooth without defects. Additionally, calcined phosphogypsum exhibited the highest mechanical performance at w/c = 0.70. This study provides new ideas for the resource utilization of waste gypsum and is of great significance for promoting the development of intelligent construction technology.


1 INTRODUCTION

Phosphogypsum is a solid waste generated by phosphochemical enterprises in the production of phosphoric acid fertilizers (Tayibi et al., 2009). Statistics show that for every 1 ton of phosphoric acid produced globally, 4.5 to 5.5 tons of phosphogypsum is generated (Shakor et al., 2020). The composition of phosphogypsum is similar to that of natural gypsum, with $\text{CaSO}_4 \cdot 2\text{H}_2\text{O}$ accounting for more than 90% (Sun et al., 2023). Its chemical composition is influenced by the composition of phosphate ore and production processes, often containing fluorides, water-soluble phosphates, heavy metals, and other harmful substances, and it has a strong acidity (Wu et al., 2022). It may also contain radioactive elements such as radium and thorium (Xiao et al., 2021). It is

hygroscopic and can react with water to form acidic solutions (Yuvaraj et al., 2021). The long-term stacking of phosphogypsum not only occupies a large amount of land resources but also poses a serious threat to regional ecological safety (Zhang et al., 2021). These issues exert great pressure on the long-term development of China's phosphochemical industry (Zhang et al., 2019). Therefore, it is necessary to promote the comprehensive utilization of phosphogypsum and improve the level of resource utilization technology (Zhang et al., 2020). Provinces(cities) are actively promoting the resource utilization of phosphogypsum (Zhao et al., 2020; Zhou et al., 2023; Rashad, 2017), based on which, various new types of building materials are continuously innovated and transformed, striving to achieve sustainable development.

^a <https://orcid.org/0009-0003-9136-9208>

^b <https://orcid.org/0009-0009-6501-8950>

^c <https://orcid.org/0000-0002-9556-6765>

At the same time, with the rapid development of urbanization and intelligent industries worldwide, 3D printing technology has become a global research and application hotspot. 3D printing concrete technology has characteristics such as low construction costs, free structural design, high molding precision, low construction noise, and less dust pollution, playing an irreplaceable role in the transformation and upgrading of China's construction industry.

In this study, we systematically investigated the impact of different calcination temperatures on the dehydration reaction, phase transformation, and mechanical properties of phosphogypsum, and further explored the influence of w/c on the morphology, structure, and strength of phosphogypsum hydration products. In addition, this paper also assessed the feasibility of 3D printing of phosphogypsum, providing new ideas for the application of phosphogypsum in the construction field. Through this study, we aim to provide a scientific basis for the high-value utilization of phosphogypsum, promote the transformation of phosphogypsum from waste to resources, and contribute to environmental protection and sustainable development.

2 METHOD

2.1 Raw Materials

Phosphogypsum, a byproduct generated during phosphoric acid production, served as the primary material in this investigation. Predominantly comprised of $\text{CaSO}_4 \cdot 2\text{H}_2\text{O}$, PG also contains impurities like phosphorus oxide and silica. The chemical composition of the initial PG sample was assessed using a Rigaku ZSX Primus IV XRF spectrometer, with the findings detailed in Table 1. Qualitative analysis of the phase composition of the original PG was conducted using XRD. Notably, distinct peaks were observed in the X-ray diffraction

pattern within the 10° - 30° 2θ range, as depicted in Figure 1. The morphology of the initial phosphogypsum was examined through SEM. The crystal structure of phosphogypsum primarily exhibited rhombus or parallelogram plate shapes, with fine granular and flocculent impurities adhering to the surface, as illustrated in Figure 2.

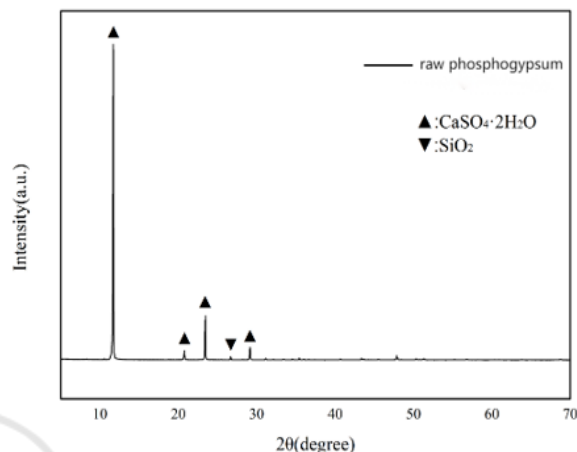


Figure 1: XRD of Phosphogypsum.

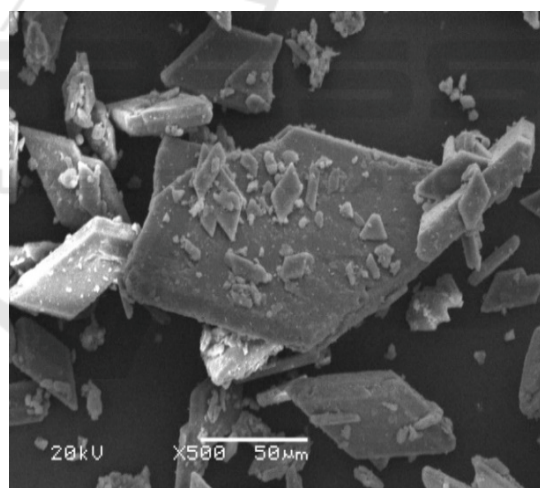


Figure 2: SEM of Phosphogypsum.

Table 1: Chemical composition of gypsum.

Sample	SO_3	CaO	SiO_2	P_2O_5	Al_2O_3	K_2O	MgO	F	Cl
PG/%	43.40	33.28	6.4	0.71	1.04	0.29	0.16	0.33	0.035

2.2 Method

This study investigates a low-energy pretreatment approach to efficiently eliminate impurities and alter the composition of phosphogypsum to increase its

utility. Calcination is chosen as the pretreatment technique, employing an SX2-4-10A muffle furnace. The calcination process involves controlling the temperature to dehydrate the dihydrate gypsum in phosphogypsum, converting it into hemihydrate

gypsum and anhydrous gypsum. Specifically, calcination temperatures of 150°C, 175°C, 200°C, 225°C, and 250°C are utilized.

In this experiment, a small gantry integrated concrete rapid-setting 3D printing equipment with mixing and extruding functions as shown in the figure was used. The pipeline of this equipment is not for conveying mixed slurry, but separates the dry material and liquid material conveying routes to achieve dedicated pipe usage, and eliminates the pumping device found in conventional 3D printing equipment. Unlike conventional mixing methods, dry materials and water can come into contact and mix rapidly in the air within the printing system, allowing materials such as phosphogypsum powder to undergo hydration reactions quickly. The work of material mixing, stirring, and extruding molding is all completed within the printing system. This ensures that the material can enter the wet extrusion from dry powder, thereby breaking through the problem that cement-based materials cannot be pumped and extruded due to short setting times. In this experiment, the water temperature was controlled between 15°C and 20°C, and different w/c were set, such as 1:1, 1.5:1, 2:1, 4:1, etc. The 3D printer was used to strictly follow the standard ratios.

A TG test was conducted using a TGA/DSC 1 thermal analyzer from the STARe system by METTER TOLEDO Group to measure the mass change of samples with temperature under programmed temperature control. The phase composition of PG was determined using XRD. Hydration kinetics of PG were investigated using a TAM air C80 isothermal calorimeter at a constant temperature of 25°C and a water/cement ratio of 4. Compressive and flexural strengths of PG were assessed using a DYE-300S computerized constant stress testing machine from Wuxi Huaxi Building Materials Testing Instrument Co., Ltd., with sample dimensions of 20mm × 20mm × 20mm and 40mm × 40mm × 160mm, respectively. The microstructure of the samples was analyzed using a Zeiss SUPRA 55 field emission SEM. Printability of PG was evaluated with an architectural 3D printer, where the water-cement ratio of printed components was adjusted by controlling water output while maintaining a consistent discharge speed.

3 RESULT

3.1 Thermal Analysis Characterization

Figure 3 illustrates the thermogravimetric analysis of PG. The dehydration process of PG initiates at approximately 100°C, with a gradual release of water until around 300°C, marking the completion of dehydration, resulting in a weight loss of approximately 19.5%. The derivative thermogravimetric (DTG) curve displays two distinct dehydration peaks. The first peak, occurring between 100°C and 166°C with a peak at 157°C, corresponds to an initial mass loss of 14.7%. The second peak, observed between 157°C and 300°C with a peak at 175°C, corresponds to an initial mass loss of 4.8%. The transformation of $\text{CaSO}_4 \cdot 2\text{H}_2\text{O}$ to $\text{CaSO}_4 \cdot 1/2\text{H}_2\text{O}$ involves the removal of 1.5H₂O in the first stage, followed by the conversion of CaSO_4 to $\text{CaSO}_4 \cdot 1/2\text{H}_2\text{O}$ by eliminating the remaining 1/2H₂O in the second stage.

3.2 XRD

Figure 4(a) shows the XRD patterns of the PG sample at different calcination temperatures ranging from 150°C to 250°C. When 2θ is 11.7°, 14.8° and 38.3°, respectively, the diffraction peak falls on the peak with the largest difference between $\text{CaSO}_4 \cdot 2\text{H}_2\text{O}$ and $\text{CaSO}_4 \cdot 1/2\text{H}_2\text{O}$ and CaSO_4 . As can be seen from Figure 4(b), (c) and (d), when 2θ is 11.7°C, the diffraction peak decreases gradually with the increase of calcination temperature, and the diffraction peak disappears when the calcination temperature reaches 175°C. It can be concluded that $\text{CaSO}_4 \cdot 2\text{H}_2\text{O}$ is gradually depleted after the calcination temperature of the sample reaches 175°C, and the sample is mainly composed of $\text{CaSO}_4 \cdot 1/2\text{H}_2\text{O}$. In addition, when 2θ is 14.8° and 29.7°, the diffraction peak of PG increases first and then decreases with the increase of calcination temperature, and reaches the maximum value when the calcination temperature is 200°C, which may be due to the fact that the $\text{CaSO}_4 \cdot 1/2\text{H}_2\text{O}$ content of the sample first increases and then decreases, and the $\text{CaSO}_4 \cdot 1/2\text{H}_2\text{O}$ content reaches the maximum value at 200°C, and then the content gradually decreases, and with the increase of temperature, the content of CaSO_4 gradually increases, when the calcination temperature is 250°C, The diffraction peak appears at $2\theta=38.3^\circ$, and the sample is a mixture of $\text{CaSO}_4 \cdot 1/2\text{H}_2\text{O}$ and CaSO_4 .

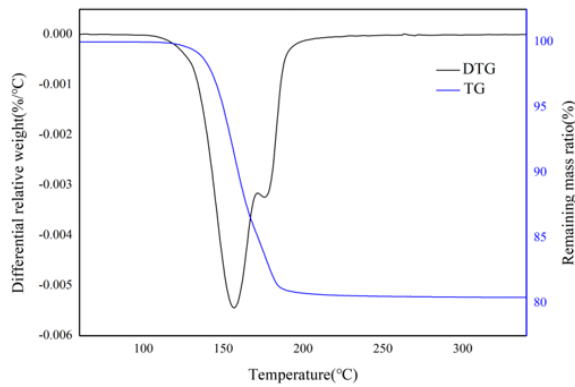


Figure 3: TG-DTG curves of the original PG.

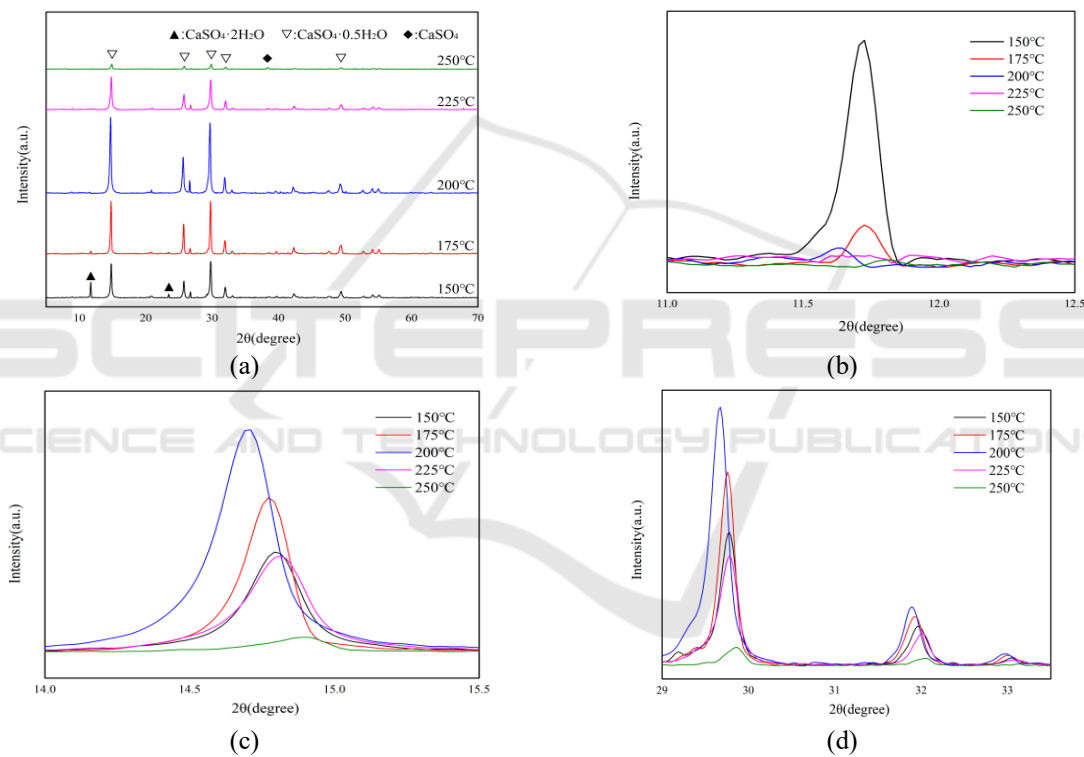


Figure 4: XRD patterns of PG at different calcination temperatures.

3.3 Compressive Strength and Flexural Strength

Figure 5 illustrates the 7-day compressive and flexural strength of calcined PG under varying water-to-ash ratios. The intensity of PG initially rises and then declines as the water-to-ash ratio increases. For ratios below 0.70, both compressive and flexural strength of PG increase with the ratio. At a ratio of 0.70, peak values are reached at 15.62 MPa and 3.86 MPa for compressive and flexural strength,

respectively. Beyond a ratio of 0.70, both strengths decrease. Specifically, at a ratio of 0.85, compressive and flexural strengths are 28.87% and 27.20% lower than those at a ratio of 0.70, measuring 11.11 MPa and 2.81 MPa, respectively. The highest hydration rate for calcined PG is observed at a water-to-ash ratio of 0.70, indicating a direct correlation between hydration level and strength. Excessive hydration beyond this ratio leads to increased formation of pores and microcracks within the material,

consequently diminishing its overall strength and stability.

3.4 SEM

Figure 6 shows SEM photos of phosphogypsum after natural curing for 7 days under different water-cement ratio conditions. The strength of PG is provided by the molecular forces connected to each other through crystal contact. From the SEM cross-sectional image with a magnification of two thousand times, it can be seen that the microstructure of the dihydrate PG crystal is relatively clear, the internal morphology and lines are disordered, and the large crystals. The gaps between them are filled with small crystals or small granular substances. When the water-cement ratio is less than or equal to 0.70, PG mainly takes the form of strips or needles after hydration. The particles are cemented together and interlaced to form a network structure. As the water-cement ratio gradually increases, the structure becomes loose and porous. There are obvious cracks in the cross section. This should be the reason why

low water-cement ratio has higher strength compared with high water-cement ratio.

3.5 The Printability

Figure 7 illustrates the printing effects of calcined phosphogypsum (PG) under varying water-cement ratios of 0.60, 0.65, 0.67, and 0.70. In (a), at a water-cement ratio of 0.60, the PG slurry exhibits severely restricted fluidity, leading to discontinuous extrusion, material breaks, and uneven surfaces with significant cracking. Increasing the water-cement ratio to 0.65 (b) reduces cracking but results in a rough surface with noticeable flaws. At a ratio of 0.67 (c), the printing quality improves markedly, with continuous and uniform extrusion, and a smooth, flawless surface. However, at 0.70 (d), the slurry becomes excessively fluid, failing to maintain structural integrity and preventing the formation of viable printed components. These findings indicate that calcined PG slurry is printable, with a water-cement ratio of 0.67 being optimal for achieving continuous, uniform, and smooth printed structures.

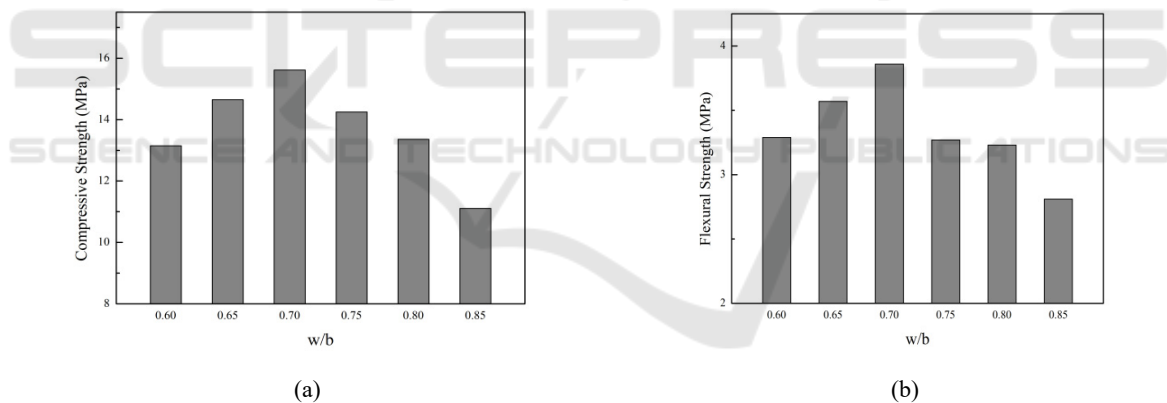
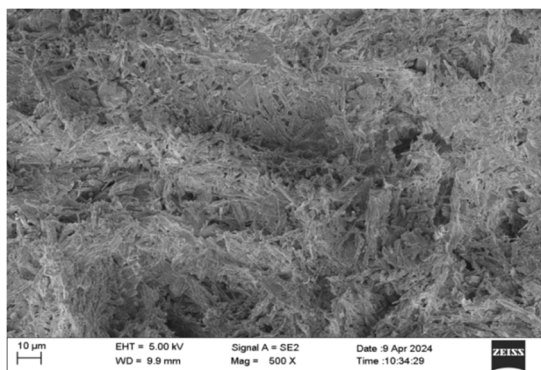
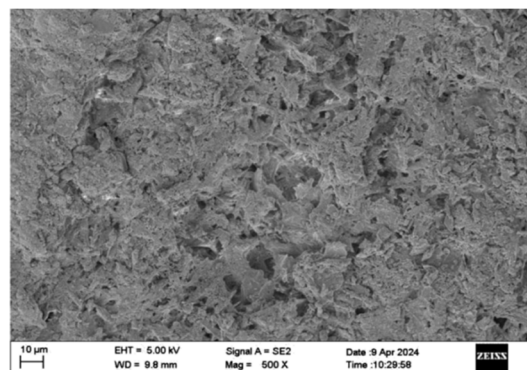


Figure 5: 7d compressive and flexural strength of PG naturally cured: (a) compressive strength (b) flexural strength.



(a) w/c = 0.65



(b) w/c = 0.70

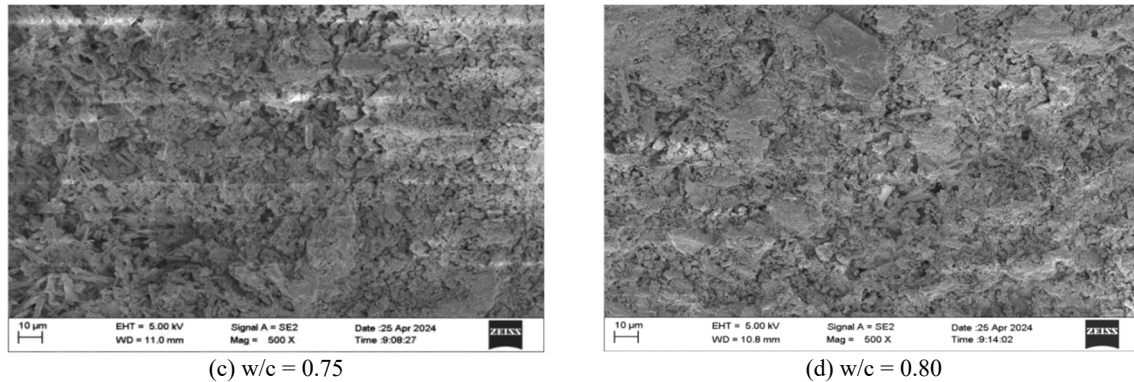


Figure 6: SEM images of phosphogypsum under different w/c at 7 days.

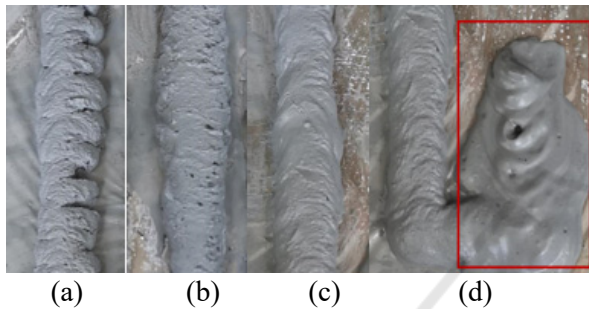


Figure 7: Printing effects of calcined PG under different water-cement ratios: (a) w/c = 0.60 (b) w/c = 0.65 (c) w/c = 0.67 (d) w/c = 0.70.

4 CONCLUSION

(1) Effect of calcination temperature on XRD pattern of PG sample. With the increase of calcination temperature, part of $\text{CaSO}_4 \cdot 2\text{H}_2\text{O}$ in PG is dehydrated to $\text{CaSO}_4 \cdot 1/2\text{H}_2\text{O}$ at 157°C , and $\text{CaSO}_4 \cdot 1/2\text{H}_2\text{O}$ may be transformed into CaSO_4 when the temperature reaches 175°C . Finally, the optimum heat treatment temperature of phosphogypsum is determined to be 175°C .

(2) The mechanical properties of calcined phosphogypsum increase and then decrease with the increase of water ash ratio. And the mechanical properties of phosphogypsum are the highest when the water ash ratio is 0.70 (the compressive strength and folding strength are 3.86MPa and 15.62MPa respectively).

(3) The shape of hydration products gradually changed from strip cross network to lamella gradually to paste, the structure changed from dense to loose and porous, and the fracture appeared obvious cracks.

(4) The calcined phosphogypsum slurry is printable, and the 3D printing effect of the slurry is best when the w/c is 0.67. The printed components are

continuous and uniform, and the surface is smooth and flawless.

REFERENCES

- Shakor, P., Nejadi, S., Paul, G., Sanjayan, J. 2020. Dimensional accuracy, flowability, wettability, and porosity in inkjet 3DP for gypsum and cement mortar materials. *Automation in Construction*, 110: 102964.
- Sun, T., Li, W., Xu, F., Yu, Z., Wang, Z., Ouyang, G., Xu, D. 2023. A new eco-friendly concrete made of high content phosphogypsum based aggregates and binder: Mechanical properties and environmental benefits. *Journal of Cleaner Production*, 400: 136555.
- Tayibi, H., Choura, M., López, F.A., Alguacil, F.J., López-Delgado, A. 2009. Environmental impact and management of phosphogypsum. *Journal of Environmental Management*, 90: 2377–2386.
- Wu, F., Ren, Y., Qu, G., Liu, S., Chen, B., Liu, X., Zhao, C., Li, J. 2022. Utilization path of bulk industrial solid waste: A review on the multi-directional resource utilization path of phosphogypsum. *Journal of Environmental Management*, 313: 114957.
- Xiao, J., Ji, G., Zhang, Y., Ma, G., Mechtcherine, V., Pan, J., Wang, L., Ding, T., Duan, Z., Du, S. 2021. Large-scale 3D printing concrete technology: Current status and future opportunities. *Cement and Concrete Composites*, 122: 104115.
- Yuvaraj, K., Mohamed Ismail, A., Nagarajan, P., Vigneshwaran, S. 2021. Design and fabrication of gypsum prototypes based on binder jetting technology. *Materials Today: Proceedings*, 45: 3085–3090.
- Zhang, C., Nerella, V.N., Krishna, A., Wang, S., Zhang, Y., Mechtcherine, V., Banthia, N. 2021. Mix design concepts for 3D printable concrete: A review. *Cement and Concrete Composites*, 122: 104155.
- Zhang, J., Tan, H., He, X., Yang, W., Deng, X., Su, Y., Yang, J. 2019. Compressive strength and hydration process of ground granulated blast furnace slag-waste gypsum system managed by wet grinding. *Construction and Building Materials*, 228: 116777.

- Zhang, Y., Yang, J., Cao, X. 2020. Effects of several retarders on setting time and strength of building gypsum. *Construction and Building Materials*, 240: 117927.
- Zhao, Y., Gao, J., Liu, C., Chen, X., Xu, Z. 2020. The particle-size effect of waste clay brick powder on its pozzolanic activity and properties of blended cement. *Journal of Cleaner Production*, 242: 118521.
- Zhou, S., Lu, Y., Pan, Y., Li, J., Qu, F., Luo, Z., Li, W. 2023. Flowability prediction of recycled α -hemihydrate gypsum for 3D powder printing under combined effects of different glidants using response surface methodology. *Developments in the Built Environment*, 16: 100265.
- Rashad, A.M. 2017. Phosphogypsum as a construction material. *Journal of Cleaner Production*, 166: 732–743.

